AIAA Propulsion and Energy Forum
July 9-11, 2018, Cincinnati, Ohio
2018 Joint Propulsion Conference

10.2514/6.2018-4970

Linear Burn Rate of Monopropellant for Multi-Mode Micropropulsion

Alex J. Mundahl*
Missouri University of Science and Technology, Rolla, Missouri 65409, United States of America

Steven P. Berg† and Joshua L. Rovey‡
University of Illinois at Urbana-Champaign, Urbana, Illinois 61801, United States of America

Multi-mode micropropulsion is a technology that can enable rapidly composable small satellites with unprecedented mission flexibility. To maximize mission flexibility a multi-mode micropropulsion monopropellant must be shared between the chemical and electric propulsion modes. Previous research has identified a promising monopropellant that is both readily catalytically exothermically decomposed (chemical mode) and electrosprayable (electric mode). In this work the linear burn rate of this monopropellant is determined and used to aid the design of a microtube catalytic chemical thruster. Experiments with a pressurized fixed volume reactor are used to determine the linear burn rate. Benchmark experiments use a 13-molar mixture of hydroxylammonium nitrate and water and show agreement to within 5% of literature data. The multi-mode monopropellant is a double-salt ionic liquid consisting of 41% 1-ethyl-3-methylimidazolium ethyl sulfate and 59% hydroxylammonium nitrate by mass. At the design pressure of 1.5 MPa the linear burn rate of this propellant is 26.4 ± 2.5 mm/s. Based on this result, the minimum flow rate required for a microtube with a 0.1 mm inner diameter within the pressure range tested is between 0.12 and 0.35 mg/s.

Nomenclature

r_b	=	linear burn rate [mm/s]
D_c	=	Diameter of propellant container [cm]
D_t	=	Diameter of microtube [cm]
m_p	=	mass of propellant used [g]
$\dot{m}_p$	=	mass flow rate of propellant [mg/s]
Δh	=	change in height of propellant sample [mm]
Δt	=	change in time [s]
ρ_p	=	density of propellant used [g/cm^3]

I. Introduction

MULTI-mode propulsion is the use of two or more integrated, yet fundamentally different propulsive modes on a single spacecraft. Recently proposed systems make use of a high-specific impulse, usually electric mode, and a high-thrust, usually chemical mode. This can be beneficial in two primary ways: an increase in mission flexibility,[1-5] and the potential to design a more efficient orbit [6-9]. An increase in mission flexibility is achieved due to the availability of the two differing propulsive maneuvers to the mission designer at any point during the mission. This

* Graduate Research Assistant, Aerospace Plasma Laboratory, Mechanical and Aerospace Engineering, 160 Toomey Hall, 400 W. 13th Street, Student Member AIAA.
† Intelligence Community Postdoctoral Fellow, Department of Aerospace Engineering, Talbot Laboratory, 104 South Wright Street, Senior Member AIAA.
‡ Associate Professor of Aerospace Engineering, Department of Aerospace Engineering, 317 Talbot Laboratory, 104 South Wright Street, Associate Fellow AIAA.

allows for drastic changes to the mission thrust profile at virtually any time before or even after launch without the need to integrate an entirely new propulsion system. Additionally, it has been shown that under certain mission scenarios it is beneficial in terms of spacecraft mass savings, or deliverable payload, to utilize separate high-specific impulse and high-thrust propulsion systems even in hybrid propulsion systems [6, 8, 10]. However, even greater mass savings can be realized by using a shared propellant and/or hardware, even if the thrusters perform lower than state-of-the-art in either mode [3, 11]. In order to realize the full potential of a multi-mode propulsion system, it is necessary to utilize one shared propellant for both modes; this allows for a large range of possible maneuvers while still allowing for all propellant to be consumed regardless of the specific choice or order of maneuvers [4].

Small spacecraft have seen a growth in popularity, specifically microsatellites (10-100 kg) and nanosatellites (1-10 kg), including the subset of CubeSats. Many different types of thrusters have been proposed to meet the demanding requirements placed on spacecraft of this type. Electrospray propulsion systems are good options for micropropulsion, and have been selected for such applications [12, 13]. Many different chemical propulsion systems have also been proposed, including a microtube-based system [14-17]. This propulsion system utilizes a heated tube with a typical diameter of 1 mm or less, and may have a catalytic surface material. These microtubes can also be used as the capillary type emitters in electrospray propulsion systems. Therefore, this microtube geometry was chosen for the proposed multi-mode propulsive system with only one propellant [5, 18-22].

Recent efforts in developing monopropellants for space vehicles have focused on finding a high-performance, low-toxicity propellant replacement for traditional, but highly toxic options. Hydrazine has been chosen for use in gas generators and spacecraft monopropellant thrusters due to its storability and favorable decomposition characteristics that provide relatively high performance [23]. However, hydrazine is difficult from a handling perspective since it is highly toxic. A large amount of the research toward a hydrazine replacement is focused on energetic ionic liquids. An energetic ionic liquid is a molten salt with an energetic functional group capable of rapid exothermic decomposition. Energetic salts that have been studied for such purposes include ammonium dinitramide (ADN), hydrazinium nitroformate (HNF), and hydroxylammonium nitrate (HAN) [23-33]. Typically, these salts are mixed with compatible fuels to improve the performance characteristics of the propellant. However, the high combustion temperatures for these energetic monopropellants have been the main limitation in their practical use in spacecraft thrusters, but recent research in thermal management and materials have mitigated some issues, and multiple flight tests are scheduled, or have already been conducted [12, 33, 34]. These propellants perform well in chemical thrusters, but they are fundamentally unable to perform as an electrospray propellant due to their water content or other volatile component. To overcome this, two propellants have been developed that can function as both a chemical monopropellant and an electrospray propellant [11]. These monopropellants have been previously synthesized and assessed for thermal and catalytic decomposition within a microreactor,[35] and for high performance in an electrospray emitter [18]. One of the monopropellant combinations, a mixture of 1-ethyl-3-methylimidazolium ethyl sulfate ([Emim][EtSO4]) and hydroxylammonium nitrate (HAN), has also been further analyzed to determine its decomposition characteristics on relevant catalytic surfaces [19, 35, 36]. This paper further studies the characteristics of the [Emim][EtSO4]-HAN monopropellant by determining the linear burn rate of this propellant at pressures relevant to typical monopropellant thruster operation [20, 21].the previously described monopropellants were developed, synthesized, and shown to be capable of high performance in an electrospray thruster [11, 18].

The linear burn rate of the propellant used at the thruster's anticipated operating pressures is a useful parameter in the design of the system, both for thruster operation and flashback prevention. The linear burn rate has been studied previously for monopropellants, including HAN-based monopropellants [37-40]. This paper presents results on the experimental determination and assessment of the linear burn rate characteristics of the [Emim][EtSO4]-HAN propellant at various pressures using a pressurized strand burner setup. These measurements, taken together, can be used to aid in the design and optimization of a catalytic microtube thruster. Section II describes the setup of the experiment, Section III presents the results, Section IV discusses these results including relevant development and selection of microtube thruster parameters, and Section V presents the conclusions of this study.

II. Experimental Setup

The pressurized linear burn rate studies performed here are similar to previous studies utilizing nitromethane or HAN-based monopropellants [41, 42]. In a pressurized linear burn rate experiment a sample of propellant ignites and combusts within a known sealed volume, and pressure within the volume is measured as a function of time. The determined burn time of the propellant sample is based on the discontinuities within the pressure profile corresponding to the initiation and extinguishment of combustion. The linear burn rate of the propellant sample is calculated by utilizing the measured burn time, mass of the propellant sample, and the sample holder's geometry.

Benchmark tests using 13M HAN-water are conducted, followed by tests using the [Emim][$EtSO_4$]-HAN monopropellant. The monopropellant has a mixture ratio of 41% [Emim][$EtSO_4$] to 59% HAN by mass and is the focus of previous research [4, 5, 11, 18, 20, 35]. The synthesizing process for this propellant is described in detail within previous studies [5, 35, 36]. The 13M HAN-water solution was prepared by drying 24% by wt. HAN-water solution until solid HAN crystals formed, then adding distilled water to the solid HAN for the final solution. Relevant propellant characteristics are given in Table 1.

Table 1 Propellant Characteristics

Propellant Tested	ρ_p [g/cm^3]	Mass HAN [%]	Mass Other [%]
HAN-Water	1.57 [36, 43]	80	20
[Emim][$EtSO_4$]-HAN	1.53 [36, 43]	59	41

An overview of the full experimental setup is shown in Fig. 1a, and Fig. 1b shows the propellant holder stand in more detail. The propellant sample holder, location A in Fig. 1b, is a 5.9 mm internal-diameter, 45 mm tall quartz tube with a quartz cylinder as the base. The propellant holder dimensions allow each test to use 1 mL of propellant. For each test, two pieces of equal length 30-gauge nickel-chromium (nichrome) wire were twisted together and soldered to the electrical leads within the propellant holder stand. The nichrome wires are then bent and submerged within the propellant no more than 5% of the total height of the internal volume available within the propellant holder (~2.25mm). This is demonstrated at location B in Fig. 1b. Two Solid Sealing Technology 1.27 mm diameter copper feedthroughs served as the electrical feedthroughs providing power to ignite the propellant. These electrical feedthroughs are at locations 1 and C in Fig. 1a and Fig. 1b respectively. The propellant holder stand, shown at location 2 in Fig. 1a, attaches to the top flange of the pressure vessel via four threaded rods. The top flange, location 3 in Fig. 1a, connects to the stainless-steel pressure vessel, location 4 in Fig. 1a, with an approximate volume of 2L. The pressure vessel was sized to optimize the trade between minimizing the pressure range within each test and having a notable pressure increase for burn time calculations. The top flange of the pressure vessel also connects to an Omega PX309-1KA5V pressure transducer, location 5 in Fig. 1a, with an absolute pressure range of 0 to 6.89 MPa. This transducer monitors the pressure versus time within the volume. The environment control system, location 6 in Fig. 1a, contains multiple valves to control the internal environment of the pressure vessel. These valves open the volume to the laboratory exhaust system, location 7 in Fig. 1a, the mechanical vacuum pump to evacuate the pressure vessel, location 8 in Fig. 1a, or the laboratory's inert argon supply to pressurize the evacuated system to the desired test pressure, location 9 in Fig. 1a.

a).

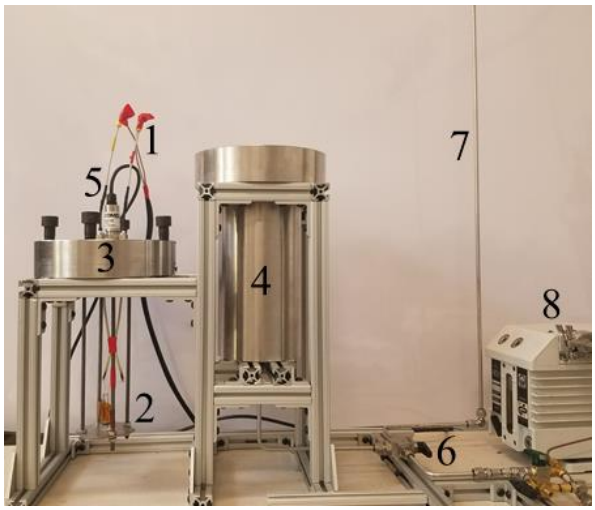

b).

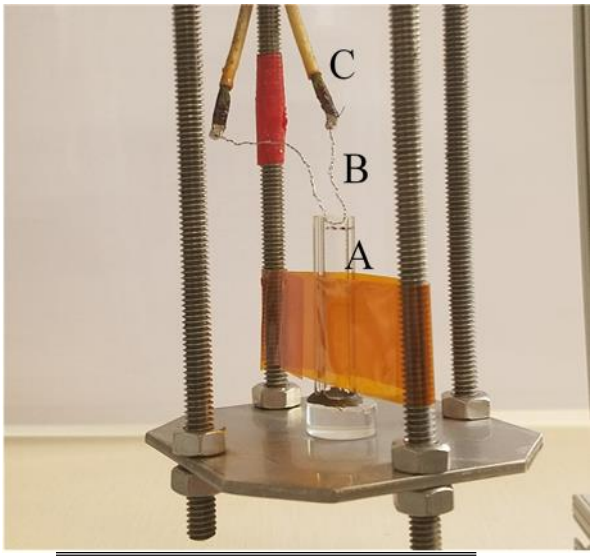

Legend	
1).	Electrical Feedthrough
2).	Propellant Holder Stand
3).	Top Flange
4).	Pressure Vessel
5).	Pressure Transducer
6).	Environment Control System
7).	Exhaust System
8).	Vacuum Pump
A).	Propellant Sample Holder
B).	Nichrome Wire
C).	Electrical Feedthrough

Fig. 1 Experimental setup. a). General setup b). Propellant holder stand

The experimental procedure starts with soldering the nichrome wire to the electrical feedthroughs. Then, a Torbal AGC500 mass balance with 0.001 gram resolution is used to determine the mass of the propellant holder before and directly after filling the holder with the propellant sample. Afterwards, the propellant holder is placed on the propellant stand and held in place with Kapton tape. The nichrome wire is dipped in the propellant sample to the provided tolerance. The top flange is then secured to the pressure vessel, which the mechanical rough pump evacuates to a pressure less than 1.3 kPa. After reaching this reduced pressure, the volume is pressurized with argon gas to the

desired test pressure. Due to the hygroscopic nature of the propellant, the exposure time of each propellant sample to the atmosphere was limited to five minutes. The results presented below are for a pressure range of 0.45 to 1.48 MPa because this is the pressure range envisioned for a multi-mode micropropulsion system designed for small satellites [5]. Once the system reaches the desired pressure, the Sorensen DLM 20-30 power supply applies 8.5 A of current to the system, triggering the Tektronix DPO 2024 Digital Phosphor Oscilloscope to record the pressure transducer output and power supply voltage. The applied current resistively heats the propellant sample, and the nichrome wire to the point of breaking within 3 seconds. This is similar to previous studies [41].

III. Results

The results from the linear burn rate experiments are presented here. Initially, a set of benchmark tests are performed with 13M HAN-water propellant samples at pressures of 1.48, 2.03, and 3.14 MPa. These tests show good agreement with literature [38]. Then, tests with the energetic ionic liquid monopropellant [Emim][$EtSO_4$]-HAN are performed at pressures of 0.45, 0.79, 0.96, 1.14, 1.31, and 1.48 MPa.

A. Calculating Linear Burn Rate

The linear burn rate is the change in height of a propellant sample over a given period. Previous studies have shown that the burn time can be determined from the pressure rise due to burning propellant within a fixed volume [41]. The change in height can be determined by the propellant mass, propellant density, and diameter of the sample holder as shown in Equation (1).

$$r_b = \frac{\Delta h}{\Delta t} = \frac{4m_p}{\pi \rho_p D_c^2 \Delta t} \tag{1}$$

The measurement error induced by these variables are considered to analyze the accuracy of the results provided below. An error of ±0.003 g is possible for the propellant mass, ±0.01 g/cm^3 for the propellant density, ±0.001 mm for the inner diameter of the propellant holder, and ±0.002 seconds for the time. When applied for maximum difference from the originally calculated results, a maximum error of ±2.6% is possible. Seeing this error is less than the 3-15% variance in the results at the same pressure, a 95% confidence interval from the 3 points at each pressure provides the error bars presented below.

B. Benchmark HAN-Water Results

Tests are performed with a 13.0M HAN-water mixture and compared with previous results by Katsumi, et. al.[38] to benchmark and validate the experimental setup and test procedure. Three tests are performed at 3.14 MPa and 2.03 MPa, and one test at 1.48 MPa. A pressure profile during a 1.48 MPa test of the 13M HAN-water solution is given in Fig. 2. There is a discontinuity in the pressure profile at 0.94 seconds indicating the ignition and initiation of combustion of the propellant. The end of combustion is the discontinuity at 5.7 seconds, where the pressure profile then turns into an exponential decreasing trend. This decrease in pressure depicts the heated combustion products cooling after all the propellant has been consumed. The difference between these two points is the burn time for the sample. Within this burn time, there is a large inflection in the pressure directly prior to the end of the burn time. This inflection is found in the literature [44], which states this inflection point separates the liquid and gas phases, and the gas phase produces exothermic reactions. The two phase burning shown in Fig. 2 also corresponds with other literature discussing the two phase nature of this HAN-Water solution combustion [38], the burn rate for the 80% HAN-water mixture at 3.14 MPa is 283.5 ± 6.4 mm/s, 2.03 MPa is 124.7 ± 4.5 mm/s, and at 1.48 MPa is 8.6 mm/s using this experimental setup, and is depicted graphically in Fig. 3 with respect to the literature [38].

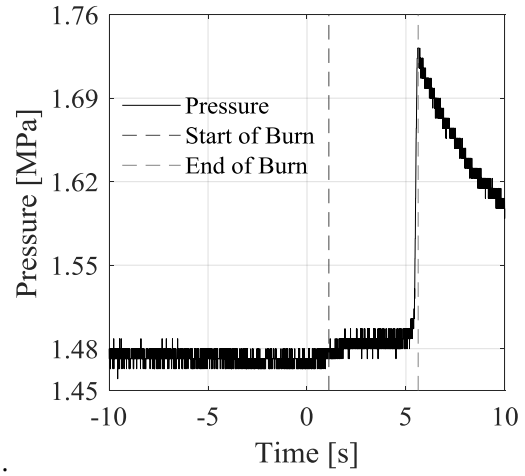

Fig. 2 HAN-water pressure vs. time at 1.48 MPa

Results from previous experiments are plotted alongside the average burn rate measured here in Fig. 3. Previous work by Katsumi et. al.[38] measured the burn rate of 80, 82.5, 85, and 90% HAN-water mixtures from 1-10 MPa. For a 80% HAN-water mixture at 1.48 MPa, Katsumi et.al.[38] measure a burn rate of 8.4 mm/s. This result is within 0.2 mm/s (<5%) of the 8.6 mm/s burn rate measured here.

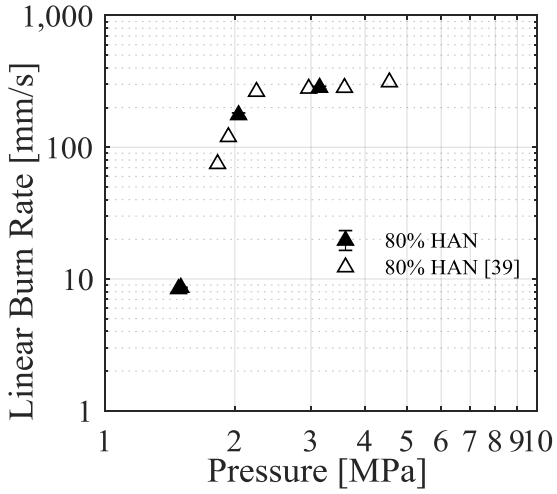

Fig. 3 Comparison of linear burn rate measured with previous results for 80% aqueous HAN solutions [38]

C. [Emim][$EtSO_4$]-HAN Monopropellant

An example pressure profile for the [Emim][$EtSO_4$]-HAN monopropellant at 1.48 MPa is shown in Fig. 4. This figure displays the start and end of the burn time, and the pressure change throughout the test. For this propellant, there is a clear increase in pressure indicating the time when the propellant sample ignites at 0.23 seconds. The [Emim][$EtSO_4$]-HAN monopropellant causes a rise in pressure of approximately 0.45 MPa. The pressure remains high until 1.9 seconds followed by an exponential pressure decrease as the system begins to stabilize back to equilibrium. The burn time determined from similar plots for each sample, along with the measured mass and calculated burn rate are displayed in Fig. 5. The average linear burn rate, determined from three tests at each starting

pressure are 26.4±2.8 mm/s, 19.7±0.9 mm/s, 10.3±0.7 mm/s, 22.4±3.5 mm/s, 18.7±2.7 mm/s and 20.0±3.9 mm/s for the starting pressures 1.48, 1.31, 1.14, 0.96, 0.79, and 0.45 MPa respectively.

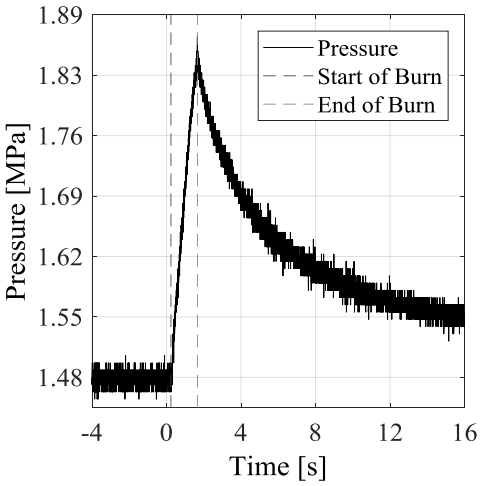

Fig. 4 [Emim][EtSO4]-HAN pressure vs. time at 1.48 MPa

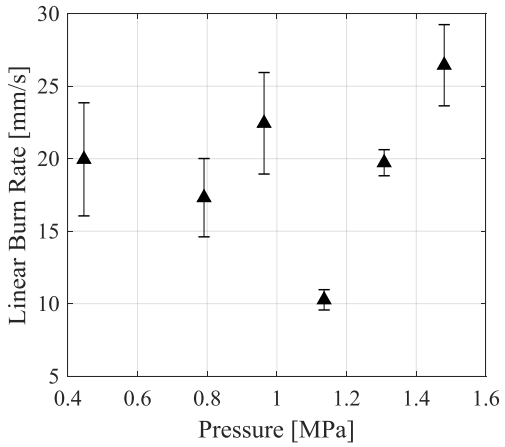

Fig. 5 [Emim][EtSO4]-HAN results at multiple pressures

IV. Discussion

Results from the preceding section are discussed, including insights for the development of a microtube thruster. The effect of pressure on the burn rate will be discussed first, followed by the effect of these results on the design of a multi-mode propulsion system.

A. Pressure Trend for HAN-based Monopropellant Burn Rate

HAN-based monopropellants have been studied previously [38, 43, 45-50]. Katsumi et. al.[38] report on a 95% by mass HAN-water mixture and show that burn rate increases with pressure for pressures above 4 MPa. A similar trend is reported for 85% HAN-water for pressure above 3.5 MPa. But at lower pressures the burn rate is approximately constant at 1.5 and 6.0 mm/s for 95% and 85% HAN-water, respectively. Amrousse et al.[45] report on monopropellant mixtures of HAN, ammonium nitrate (AN), water, and methanol named SHP163 (95/5/8/21 by moles

per reaction) and a control propellant (95/5/8/0). Results show SHP163 burn rate increases from 0.3 to 50 mm/s as pressure increases from 2 to 6 MPa. The burning rate of the control propellant increases from 7 to 300 mm/s over the same range, but for pressure below 2 MPa the burn rate is constant at 7 mm/s. Katsumi et al. [46] also report on SHP163 and the same control propellant along with another named SHP069 (95/5/8/8 by moles per reaction). Results show SHP069 burn rate increases from 3 to 200 mm/s for pressures 1.5 to 7 MPa, and for pressures less than 5 MPa the burning rate is constant at 5 mm/s. Vosen [47] reports on turbulent combustion of a mixture of HAN and triethanolammonium nitrate (TEAN) named LP1846, and 62.6% aqueous HAN solution, and shows that burn rate decreases for both propellants from about 250 mm/s to 80 mm/s as pressure increases from 6 MPa to 30 MPa. Vosen[48] also reports on the laminar burning velocity of the HAN-based liquid propellant LP1846 within the pressure range of 6.7 to 34 MPa, with results showing a laminar burning rate between 26.7 and 27.9 mm/s at pressures of 30 to 34 MPa. Vosen [49] reported on the concentration and pressure effects on aqueous HAN solution decomposition rates for mixtures of 3.12 to 13.0 molar aqueous HAN solutions over pressures of 6 to 34 MPa. This report concluded that the overall decomposition rate was a function of the pressure and the concentration of the monopropellant mixtures. Kondrikov et al.[50] reports results for crystalline HAN, monopropellant mixture of 57.5% HAN, 5% water, and 37.5% monoethanolamine nitrate (EAN), and 9.2 molar and 8.6 molar aqueous HAN solutions within the pressure range of 0.1 to 36 MPa. Results showed an increase in linear burning rate from greater than 200 to 600 mm/s in the pressure regime of 2 to 12 MPa for the monopropellant mixture of HAN, EAN, and water, and an increase in burning rate from 0.1 to 50 mm/s for the pressure range of 0.5 to 11 MPa. Mundahl et. al.[43] report on a mixture of 41% [Emim][$EtSO_4$] and 59% HAN by mass for two different heating element geometries within the pressure range of 0.5 to 1.5 MPa. A relatively constant linear burn rate is observed with an average burning rate of 41.4 mm/s for the most submerged heating element geometry.

In many HAN-based monopropellants it is observed that below a particular pressure (in most cases 2-4 MPa) the burn rate remains relatively constant, and this trend also appears to be present in the data of Fig. 5. Constant burn rate at low pressure was observed in HAN-water mixtures by Katsumi et.al. [38], HAN-AN-water mixtures by Amrousse et al. [45], and Katsumi et al. for SHP069, SHP163, and a control monopropellant mixture [46]. The data presented in Fig. 5 is for pressure below 1.5 MPa and exhibits an almost constant trend with pressure. Across all pressures tested the average linear burn rate is 19.6 mm/s with an average deviation of about 17%. The largest difference from the average burn rate is 50% at 1.14 MPa. Still this difference is significantly less than what is observed in the literature for HAN-based monopropellants at higher pressure, where linear burn rate often increases by an order of magnitude or more. The multi-mode propellant appears to conform with many previous HAN-based monopropellants by exhibiting a nearly constant linear burn rate at low pressure with a magnitude (~20 mm/s) similar to other HAN-based monopropellants in the same pressure range (~5-50 mm/s).

The results of Fig. 5 also compare well with previous tests of the multi-mode propellant. Previous tests used a similar linear burn rate experiment, but fully dipped the nichrome wire into the propellant sample [43]. Results from those previous tests predicted linear burn rates 75% higher than those of Fig. 5. This may be expected since a fully-dipped nichrome wire would ignite the propellant everywhere in the propellant holder (as opposed to just at the surface). This would give rise to an artificially high linear burn rate as all the propellant burns at once instead of a linear progression. The burn rate measured in those tests was also nearly constant across the same pressure range tested in this analysis, 0.45 to 1.48 MPa, with an average burning rate of 41.4 mm/s. It is interesting to note that those previous results indicate a minimum burn rate at 1.14 MPa, like the results in Fig. 5.

There is a non-negligible pressure rise during the linear burn rate experiment, but maximum pressure is still well below the regime where strong pressure dependence on burn rate is expected (<2 MPa). As shown in Fig. 2 and Fig. 4, when the propellant ignites and generates gaseous products the pressure in the vessel increases by up to 25%. We report the initial pressure as the test condition, but clearly the pressure increases during the test. However, even with this pressure increase the benchmark data agree well (within 5%) with literature (Fig. 3). And as discussed in the preceding paragraph, the multi-mode propellant exhibits nearly constant burn rate with pressure within the pressure range being tested, a result that is similar to many other HAN-based monopropellants.

B. Impact of Burn Rate Results on Catalytic Microtube Microthruster Design

The linear burn rate is a useful parameter in the design of chemical monopropellant thrusters. The most obvious application to thruster design is in the prevention of flashback into the feed system or propellant tank. Since the goal of the sample holder in the linear burn rate experiments is to minimize the effect of heat transfer in the quenching of the propellant decomposition reaction, the linear burn rate results can be used to obtain an estimate of the required minimum feed rate in a tube or other geometry. A recent multi-mode concept is to integrate together a catalytic microtube with an electrospray thruster [22]. Here, we use the linear burn rate obtained from experiment to define a minimum flow rate as a function of tube diameter to feed the propellant to the catalytic microtube thruster at a rate

greater than the burn rate of the propellant. The minimum flow rate is calculated for tube inner diameters of 0.1 to 10 mm using Equation (2) and is shown in Fig. 6.

$$\dot{m}_p = \frac{\pi}{4} \rho_p r_b D_t^2 \tag{2}$$

The two lines shown in Fig. 6 correspond to the largest range of possible minimum burn rates determined for the [Emim][$EtSO_4$]-HAN propellant in the tested pressure range of 0.45 to 1.48 MPa. Using these results at 1.48 MPa, the minimum flow rate required is between 0.12 and 0.35 mg/s for a tube of 0.1 mm inner diameter and 1.16 to 3.51 g/s for a tube of 10 mm inner diameter. For a microtube type thruster, which does not include a nozzle, the specific impulse of this propellant is predicted to be 170 seconds [11]. This corresponds to a minimum thrust level between 0.19 and 0.59 mN for a 0.1 mm inner diameter tube and between 1.93 and 5.85 N for a 10 mm diameter tube. Or, stated in a way more representative of design selection, if a thruster of 1.93 to 5.85 N thrust per emitter is desired, the feed tube can be a maximum of 10 mm inner diameter. If the diameter is larger, then the mass flow rate would be too low, and the propellant would burn back into the propulsion system.

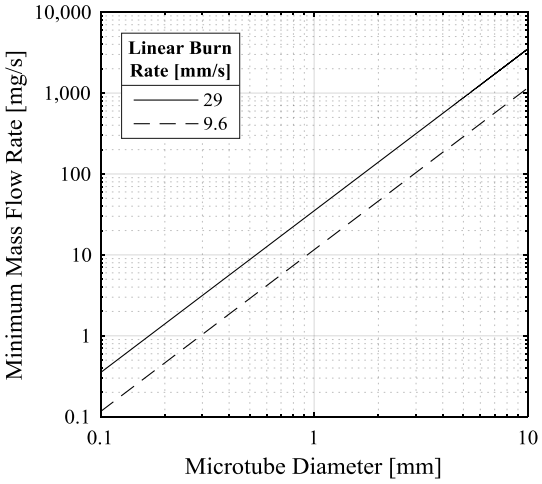

Fig. 6 Minimum required propellant mass flow rate to prevent flashback into feed system for [Emim][$EtSO_4$]-HAN propellant

V. Conclusion

From the results provided and the following discussion, it was determined that the linear burn rate of aqueous HAN solutions tested in this linear burning rate experiment are similar to the discussed literature, to within 5%. Also, it was observed that the [Emim][$EtSO_4$]-HAN monopropellant mixture is readily ignited in the pressure regime tested in this linear burn rate experiment, with a rapid pressure rise. This monopropellant mixture has linear burn rate in the pressure range tested, 0.45 to 1.48 MPa, between 9.6 and 29 mm/s with 95% confidence. From this result, it was concluded that the minimum flow rate required for a 0.1 mm microtube is between 0.12 to 0.35 mg/s, and 1.16 to 3.51 g/s for a tube of 10 mm inner diameter. These discoveries should help improve the design and operation of multi-mode micropropulsion systems.

Acknowledgments

The authors would like to thank the researchers of the Aerospace Plasma Laboratory for their assistance throughout this experiment and providing insightful information. The authors thank the technicians within the department machine shop for their assistance in the manufacturing process of this experiment. Support for this work was provided through the NASA Marshall Space Flight Center, NASA grant NNM15AA09A, and the Air Force University Nanosatellite Program through the Utah State University Research Foundation, grant CP0039814. Additional support was provided by NASA Goddard Space Flight Center through the NASA Undergraduate Student Instrument Project grant NNX16AI85A, and the University of Missouri System Fast Track Program.

References

[1] Ulybyshev, Y. P., "Optimization of Multi-Mode Rendezvous Trajectories with Constraints," *Cosmic Research*, Vol. 46, No. 2, pp. 133, 2008.
doi: 10.1134/s0010952508020056

[2] Hass, J. and Holmes, M., "Multi-Mode Propulsion System for the Expansion of Small Satellite Capabilities," NATO Rept. MP-AVT-171-05, 2010.

[3] Donius, B. R. and Rovey, J. L., "Ionic Liquid Dual-Mode Spacecraft Propulsion Assessment," *Journal of Spacecraft and Rockets*, Vol. 48, No. 1, pp. 110-123, 2011.
doi: 10.2514/1.49959

[4] Berg, S. P. and Rovey, J. L., "Assessment of High-Power Electric Multi-Mode Spacecraft Propulsion Concepts," *33rd Internation Electric Propulsion Conference*, 2013.

[5] Berg, S. P. and Rovey, J. L., "Assessment of Multimode Spacecraft Micropropulsion Systems," *Journal of Spacecraft and Rockets*, Vol. 54, No. 3, pp. 592-601, 2017.
doi: 10.2514/1.A33649

[6] Kluever, C. A., "Spacecraft Optimization with Combined Chemical-Electric Propulsion," *Journal of Spacecraft and Rockets*, Vol. 32, No. 2, pp. 378-379, 1995.
doi: 10.2514/3.26623

[7] Kluever, C. A., "Optimal Geostationary Orbit Transfers Using Onboard Chemical-Electric Propulsion," *Journal of Spacecraft and Rockets*, Vol. 49, No. 6, pp. 1174-1182, 2012.
doi: 10.2514/1.A32213

[8] Oh, D. Y., Randolph, T., Kimbrel, S. and Martinez-Sanchez, M., "End-to-End Optimization of Chemical-Electric Orbit-Raising Missions," *Journal of Spacecraft and Rockets*, Vol. 41, No. 5, pp. 831-839, 2004.
doi: 10.2514/1.13096

[9] Oleson, S. R., Myers, R. M., Kluever, C. A., Riehl, J. P. and Curran, F. M., "Advanced Propulsion for Geostationary Orbit Insertion and North-South Station Keeping," *Journal of Spacecraft and Rockets*, Vol. 34, No. 1, pp. 22-28, 1997.
doi: 10.2514/2.3187

[10] Mailhe, L. M. and Heister, S. D., "Design of a Hybrid Chemical/Electric Propulsion Orbital Transfer Vehicle," *Journal of Spacecraft and Rockets*, Vol. 39, No. 1, pp. 131-139, 2002.
doi: 10.2514/2.3791

[11] Berg, S. P. and Rovey, J. L., "Assessment of Imidazole-Based Ionic Liquids as Dual-Mode Spacecraft Propellants," *Journal of Propulsion and Power*, Vol. 29, No. 2, pp. 339-351, 2013.
doi: 10.2514/1.B34341

[12] Chiu, Y.-H. and Dressler, R. A., "Ionic Liquids for Space Propulsion," ACS Publications, Washington, D. C., 2007.

[13] Gamero-Castaño, M., "Characterization of a Six-Emitter Colloid Thruster Using a Torsional Balance," *Journal of Propulsion and Power*, Vol. 20, No. 4, pp. 736-741, 2004.
doi: 10.2514/1.2470

[14] Mento, C. A., Sung, C.-J., Ibarreta, A. F. and Schneider, S. J., "Catalyzed Ignition of Using Methane/Hydrogen Fuel in a Microtube for Microthruster Applications," *Journal of Propulsion and Power*, Vol. 25, No. 6, pp. 1203-1210, 2009.
doi: 10.2514/6.2006-4871

[15] Chao, Y.-C., Chen, G.-B., Hsu, C.-J., Leu, T.-S., Wu, C.-Y. and Cheng, T.-S., "Operational Characteristics of Catalytic Combustion in a Platinum Microtube," *Combustion Science and Technology*, Vol. 176, No. 10, pp. 1755-1777, 2004.
doi: 10.1080/00102200490487599

[16] Chen, C.-P., Chao, Y.-C., Wu, C.-Y., Lee, J.-C. and Chen, G.-B., "Development of a Catalytic Hydrogen Micro-Propulsion System," *Combustion Science and Technology*, Vol. 178, No. 10-11, pp. 2039-2060, 2006.
doi: 10.1080/00102200600793395

[17] Volchko, S. J., Sung, C.-J., Huang, Y. and Schneider, S. J., "Catalytic Combustion of Rich Methane/Oxygen Mixtures for Micropropulsion Applications," *Journal of Propulsion and Power*, Vol. 22, No. 3, pp. 684-693, 2006.
doi: 10.2514/1.19809

[18] Berg, S. P., Rovey, J., Prince, B., Miller, S. and Bemish, R., "Electrospray of an Energetic Ionic Liquid Monopropellant for Multi-Mode Micropropulsion Applications," *51st AIAA/SAE/ASEE Joint Propulsion Conference*, American Institute of Aeronautics and Astronautics, 2015.
doi:10.2514/6.2015-4011

[19] Berg, S. P. and Rovey, J., "Decomposition of a Double Salt Ionic Liquid Monopropellant on Heated Metallic Surfaces," *52nd AIAA/SAE/ASEE Joint Propulsion Conference*, American Institute of Aeronautics and Astronautics, 2016.
doi:10.2514/6.2016-4578

[20] Berg, S. P., "Development of Ionic Liquid Multi-Mode Spacecraft Micropropulsion Systems," Dissertation, Mechanical and Aerospace Department, Missouri University of Science and Technology, 2015.

[21] Berg, S. P. and Rovey, J., "Decomposition of a Double Salt Ionic Liquid Monopropellant in a Microtube for Multi-Mode Micropropulsion Applications," *53rd AIAA/SAE/ASEE Joint Propulsion Conference*, American Institute of Aeronautics and Astronautics, 2017.
doi:10.2514/6.2017-4755

[22] Berg, S. P. and Rovey, J. L., "Design and Development of a Multi-Mode Monopropellant Electrospray Mircropropulsion System," *30th AIAA/USU Conference on Small Satellites*, to be presented, 2016.

[23] George, P. S. and Oscar, B., "Rocket Propulsion Elements," Wiley, New York, 2001.

[24] Courthéoux, L., Amariei, D., Rossignol, S. and Kappenstein, C., "Thermal and Catalytic Decomposition of Hnf and Han Liquid Ionic as Propellants," *Applied Catalysis B: Environmental*, Vol. 62, No. 3, pp. 217-225, 2006.
doi: 10.1016/j.apcatb.2005.07.016

[25] Yu, Y.-S., Li, G.-X., Zhang, T., Chen, J. and Wang, M., "Effects of Catalyst-Bed's Structure Parameters on Decomposition and Combustion Characteristics of an Ammonium Dinitramide (Adn)-Based Thruster," *Energy Conversion and Management*, Vol. 106, No. pp. 566-575, 2015.
doi: 10.1016/j.enconman.2015.09.036

[26] Gohardani, A. S., Stanojev, J., Demairé, A., Anflo, K., Persson, M., Wingborg, N. and Nilsson, C., "Green Space Propulsion: Opportunities and Prospects," *Progress in Aerospace Sciences*, Vol. 71, No. pp. 128-149, 2014.
doi: 10.1016/j.paerosci.2014.08.001

[27] Schöyer, H., Schnorhk, A., Korting, P., Va, P., Mul, J., Gadiot, G. and Meulenbrugge, J., "High-Performance Propellants Based on Hydrazinium Nitroformate," *Journal of Propulsion and Power*, Vol. 11, No. 4, pp. 856-869, 1995.
doi: 10.2514/3.23911

[28] Zhang, T., Li, G., Yu, Y., Sun, Z., Wang, M. and Chen, J., "Numerical Simulation of Ammonium Dinitramide (Adn)-Based Non-Toxic Aerospace Propellant Decomposition and Combustion in a Monopropellant Thruster," *Energy Conversion and Management*, Vol. 87, No. pp. 965-974, 2014.
doi: 10.1016/j.enconman.2014.07.074

[29] Eloirdi, R., Rossignol, S., Kappenstein, C., Duprez, D. and Pillet, N., "Design and Use of a Batch Reactor for Catalytic Decomposition of Propellants," *Journal of Propulsion and Power*, Vol. 19, No. 2, pp. 213-219, 2003.
doi: 10.2514/2.6120

[30] Farshchi, M., Vaezi, V. and Shaw, B., "Studies of Han-Based Monopropellant Droplet Combustion," *Combustion Science and Technology*, Vol. 174, No. 7, pp. 71-97, 2002.
doi: 10.1080/00102200208984088

[31] Ide, Y., Takahashi, T., Iwai, K., Nozoe, K., Habu, H. and Tokudome, S., "Potential of Adn-Based Ionic Liquid Propellant for Spacecraft Propulsion," *Procedia Engineering*, Vol. 99, No. pp. 332-337, 2015.
doi: 10.1016/j.proeng.2014.12.543

[32] Risha, G. A., Yetter, R. A. and Yang, V., "Electrolytic-Induced Decomposition and Ignition of Han-Based Liquid Monopropellants," *International Journal of Energetic Materials and Chemical Propulsion*, Vol. 6, No. 5, pp. 2007.
doi: 10.1615/IntJEnergeticMaterialsChemProp.v6.i5.30

[33] Anflo, K. and Möllerberg, R., "Flight Demonstration of New Thruster and Green Propellant Technology on the Prisma Satellite," *Acta Astronautica*, Vol. 65, No. 9, pp. 1238-1249, 2009.
doi: 10.1016/j.actaastro.2009.03.056

[34] Mclean, C. H., "Green Propellant Infusion Mission Program Development and Technology Maturation," *50th AIAA/ASME/SAE/ASEE Joint Propulsion Conference*, American Institute of Aeronautics and Astronautics, 2014.
doi:10.2514/6.2014-3481

[35] Berg, S. P. and Rovey, J. L., "Decomposition of Monopropellant Blends of Hydroxylammonium Nitrate and Imidazole-Based Ionic Liquid Fuels," *Journal of Propulsion and Power*, Vol. 29, No. 1, pp. 125-135, 2012.
doi: 10.2514/1.B34584

[36] Mundahl, A. J., Berg, S. P., Rovey, J., Huang, M., Woelk, K., Wagle, D. and Baker, G., "Characterization of a Novel Ionic Liquid Monopropellant for Multi-Mode Propulsion," *53rd AIAA/SAE/ASEE Joint Propulsion Conference*, American Institute of Aeronautics and Astronautics, 2017.
doi:10.2514/6.2017-4756

[37] Chang, Y.-P., "Combustion Behavior of Han-Based Liquid Propellants," Thesis, Mechanical Engineering, The Pennsylvania State University, 2002.

[38] Katsumi, T., Hori, K., Matsuda, R. and Inoue, T., "Combustion Wave Structure of Hydroxylammonium Nitrate Aqueous Solutions," *46th AIAA/ASME/SAE/ASEE Joint Propulsion Conference & Exhibit*, American Institute of Aeronautics and Astronautics, 2010.
doi:10.2514/6.2010-6900

[39] Katsumi, T., Kodama, H., Matsuo, T., Ogawa, H., Tsuboi, N. and Hori, K., "Combustion Characteristics of a Hydroxylammonium Nitrate Based Liquid Propellant. Combustion Mechanism and Application to Thrusters," *Combustion, Explosion, and Shock Waves*, Vol. 45, No. 4, pp. 442, 2009.

doi: 10.1007/s10573-009-0055-z
[40] Pan, Y. Z., Yu, Y. G., Zhou, Y. H. and Lu, X., "Measurement and Analysis of the Burning Rate of Han-Based Liquid Propellants," *Propellants, Explosives, Pyrotechnics*, Vol. 37, No. 4, pp. 439-444, 2012.
doi: 10.1002/prep.201100042
[41] Warren, W. C., "Experimental Techniques for the Study of Liquid Monopropellant Combustion," Thesis, Mechanical Engineering, Texas A&M University, 2012.
[42] Mccown, K. W., Demko, A. R. and Petersen, E. L., "Experimental Techniques to Study Linear Burning Rates of Heterogeneous Liquid Monopropellants," *Journal of Propulsion and Power*, Vol. 30, No. 4, pp. 1027-1037, 2014.
doi: 10.2514/1.B35093
[43] Mundahl, A., Berg, S. P. and Rovey, J., "Linear Burn Rates of Monopropellants for Multi-Mode Micropropulsion," *52nd AIAA/SAE/ASEE Joint Propulsion Conference*, American Institute of Aeronautics and Astronautics, 2016.
doi:10.2514/6.2016-4579
[44] Stahl, J. M., "Analysis of Hydroxylammonium Nitrate Burning Rates," Thesis, Texas A&M University, 2017.
[45] Amrousse, R., Katsumi, T., Azuma, N. and Hori, K., "Hydroxylammonium Nitrate (Han)-Based Green Propellant as Alternative Energy Resource for Potential Hydrazine Substitution: From Lab Scale to Pilot Plant Scale-Up," *Combustion and Flame*, Vol. 176, No. Supplement C, pp. 334-348, 2017.
doi: 10.1016/j.combustflame.2016.11.011
[46] Katsumi, T., Inoue, T., Nakatsuka, J., Hasegawa, K., Kobayashi, K., Sawai, S. and Hori, K., "Han-Based Green Propellant, Application, and Its Combustion Mechanism," *Combustion, Explosion, and Shock Waves*, Vol. 48, No. 5, pp. 536-543, 2012.
doi: 10.1134/S001050821205005X
[47] Vosen, S. R., "The Burning Rate of Hydroxylammonium Nitrate-Based Liquid Propellants," *Symposium (International) on Combustion*, Vol. 22, No. 1, pp. 1817-1825, 1989.
doi: 10.1016/S0082-0784(89)80195-X
[48] Vosen, S. R., "Hydroxylammonium Nitrate-Based Liquid Propellant Combustion-Interpretation of Strand Burner Data and the Laminar Burning Velocity," *Combustion and Flame*, Vol. 82, No. 3, pp. 376-388, 1990.
doi: 10.1016/0010-2180(90)90009-G
[49] Vosen, S. R., "Concentration and Pressure Effects on the Decomposition Rate of Aqueous Hydroxylammonium Nitrate Solutions," *Combustion Science and Technology*, Vol. 68, No. 4-6, pp. 85-99, 1989.
doi: 10.1080/00102208908924070
[50] Kondrikov, B. N., Annikov, V. É., Egorshev, V. Y. and De Luca, L. T., "Burning of Hydroxylammonium Nitrate," *Combustion, Explosion and Shock Waves*, Vol. 36, No. 1, pp. 135-145, 2000.
doi: 10.1007/BF02701522